The Astrophysical Journal, 639:510–515, 2006 March 1

IS THERE ANY EVIDENT EFFECT OF CORONAL HOLES ON GRADUAL SOLAR ENERGETIC PARTICLE EVENTS?

Chenglong Shen, Yuming Wang,[1] Pinzhong Ye, and S. Wang
CAS Key Lab of Plasma Physics, School of Earth and Space Science, University of Science and Technology of China, Hefei, Anhui 230026, China
Received 2005 March 27; accepted 2005 October 26

ABSTRACT

Gradual solar energetic particle (SEP) events are thought to be produced by shocks, which are usually driven by fast coronal mass ejections (CMEs). The strength and magnetic field configuration of the shock are considered the two most important factors for shock acceleration. Theoretically, both of these factors should be unfavorable for producing SEPs in or near coronal holes (CHs). Meanwhile, CMEs and CHs could impact each other. Thus, to answer the question whether CHs have real effects on the intensities of SEP events produced by CMEs, a statistical study is performed. First, a brightness gradient method is developed to determine CH boundaries. Using this method, CHs can be well identified, eliminating any personal bias. Then 56 front-side fast halo CMEs originating from the western hemisphere during 1997–2003 are investigated as well as their associated large CHs. It is found that neither CH proximity nor CH relative location manifests any evident effect on the proton peak fluxes of SEP events. The analysis reveals that almost all of the statistical results are significant at no more than one standard deviation, σ. Our results are consistent with the previous conclusion suggested by Kahler that SEP events can be produced in fast solar wind regions and there is no requirement for those associated CMEs to be significantly faster.

Subject headings: acceleration of particles — Sun: corona — Sun: coronal mass ejections (CMEs) — Sun: particle emission

Online material: color figure

1. INTRODUCTION

Solar energetic particle (SEP) events are one of the most important processes in space weather. Generally, SEP events have two classes: one is impulsive and the other is gradual (Cane et al. 1986; Reames 1999; Kallenrode 2003). The energetic particles in impulsive events usually come from the sites where flares occur. Rapid release of magnetic energy through magnetic field reconnections produces them. The particles in gradual events are considered to be generated at coronal/interplanetary shocks driven by fast coronal mass ejections (CMEs; e.g., Reames 1999). Statistically, gradual SEP events are larger and longer than the impulsive events. Mixed SEP events may also exist (e.g., Cane et al. 2003), in which there are both flare and shock particle components.

Shock acceleration is the main mechanism of forming gradual SEP events (Cane 1997; Reames 1999; Kallenrode 2003). The correlation between the speeds of shock drivers and SEP intensities near the Earth is significant (Reames 2000), but the scatter is also remarkable (Kahler 2001; Gopalswamy et al. 2004). The large scatter is not only because CME speeds cannot reflect the real speeds and strengths of shocks, but also because there are many other impact factors not taken into account, such as the longitudes and span angles of CMEs, the background solar wind, seed populations, the interaction between multiple CMEs, the magnetic field configurations near shocks, and so on (Cane et al. 1988; Reames 1997; Kahler 2001, 2004; Kahler & Reames 2003; Gopalswamy et al. 2004). However, in order to produce a larger SEP event for a CME, the dominant factor is that the strength of driven shock should be stronger and the magnetic field close to the shock should be more capable of trapping escaping particles for repeated acceleration.

In fast solar wind streams, driven shocks are usually weak or even difficult to produce because the MHD fast-mode wave and wind flow speeds are both higher in those regions. Thus, it is expected that the fast solar wind regions should significantly differ from the slow solar wind regions in producing gradual SEP events. Kahler (2004) statistically compared the gradual SEP events produced by shocks in fast with those produced in slow solar wind regions. However, his results suggest no significant bias against SEP production in fast-wind regions. He used the O^{+7}/O^{+6} ratios at 1 AU to distinguish these two kinds of solar wind streams, and his results showed both the existence of SEPs originating in fast-wind regions and no requirement for those associated CMEs to be significantly faster.

Fast solar wind streams primarily come from coronal holes (CHs) (Bohlin 1977; Harvey & Recely 2002). So another way to examine whether there is any effect of fast streams is to investigate the effect of CHs on CMEs in producing SEP events, which is the main purpose of this paper. There is a close relationship between CMEs and CHs. The high-speed streams from CHs might constrain the motion of CMEs (e.g., Wang et al. 2004; Gopalswamy et al. 2005), and on the other hand, the magnetic field topology evolution accompanying CMEs may change the shapes of neighboring CHs (Kahler & Hundhausen 1992; Fainshtein 2000). This point further prompts us to study whether CHs could affect CMEs in producing SEP events. The rest of this paper is organized as follows: § 2 describes how to identify CHs. Section 3 represents an exhaustive statistical analysis. Finally, we give a brief summary and conclusions in § 4.

2. DETERMINATION OF CORONAL HOLES

Conceptually, CHs are considered the low-density and low-temperature regions in the corona (e.g., Harvey & Recely 2002), from which the solar wind is fast and the magnetic field is open.

[1] Corresponding author; ymwang@ustc.edu.cn.

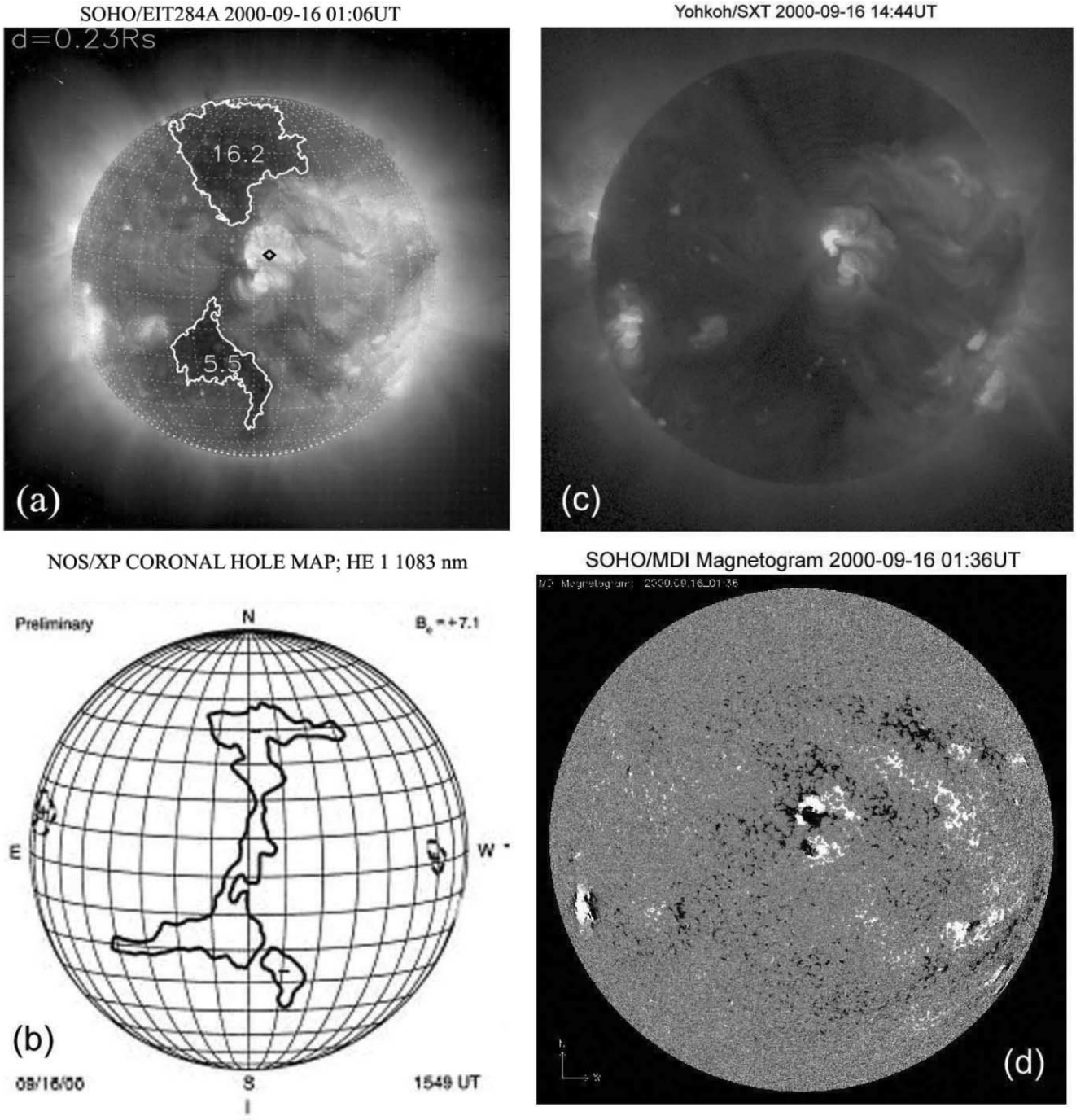

FIG. 1.—Example showing the determination of EIT 284 Å CHs. (*a*) EIT 284 Å image overplotted with the determined CH boundaries. (*b*) Kitt Peak CH map. (*c*) *Yohkoh* SXT image. (*d*) *SOHO* MDI magnetogram. [*See the electronic edition of the Journal for a color version of this figure*.]

Currently, the most widely used CH maps are provided by Kitt Peak Observatory. These so-called Kitt Peak CHs, are identified through the He 10830 Å spectral line and usually treated as the bases of CHs (Harvey & Recely 2002). Many authors use them to study the boundaries of CHs and some related phenomena (e.g., Zhao et al. 1999; Chertok et al. 2002). Soft X-ray data from the *Yohkoh* SXT instrument are also often used to study CHs. In fact, CHs were first defined as low-density and low-temperature regions in X-ray images. In addition, after the *Solar and Heliospheric Observatory* (*SOHO*) spacecraft was launched, the corona was further observed in four EUV bandpasses at Fe IX/X (171 Å), Fe XII (195 Å), Fe XV (284 Å), and He II (304 Å) by the EIT instrument (Delaboudiniere et al.1995). In different spectral lines, the appearances of CHs are somewhat different.

In this paper, we prefer using EIT 284 Å to identify CHs. This consideration is based on the following reasons.

1. EIT provides more complete observations of the corona in our study interval (from 1997 to 2003) than others.
2. Among four bands of EIT data, 284 Å observes the corona at the greatest height. Compared to the other three EIT bands, it provides the most useful coronal information for SEP acceleration. This is because near the solar surface ($\lesssim 2\ R_{\odot}$), CHs may expand rapidly and superradially with increasing height (Munro

TABLE 1

FRONT-SIDE FAST HALO CMEs ORIGINATING FROM THE WEST HEMISPHERE DURING 1997–2003

No.	CME[a]				CH			SEP	
	Date, Time	Width (deg)	Speed (km s^{-1})	Location[b] (deg)	D[c]	A[d]	P[e]	≥10 MeV[f]	≥50 MeV[g]
1	1997 Nov 6, 12:10	360	1556	S18, W62	1.1	8.3	N	490	116
2	1998 Apr 20, 10:07	165	1863	S47, W70	0.7	5.6	N	1610	103
3	1998 May 6, 8:29	190	1099	S15, W68	0.5	10.0	N	239	19.3
4	1998 Nov 5, 20:44	360	1118	N20, W23	...	...	N	...	...
5	1999 Jun 4, 7:26	150	2230	N19, W85	1.5	17.9	N	64	0.929
6	1999 Jun 28, 21:30	360	1083	N23, W42	1.1	11.6	Y	...	...
7	1999 Sep 16, 16:54	147	1021	N42, W30	...	...	N	...	...
8	2000 Feb 12, 4:31	360	1107	N13, W28	...	...	N	2.68	...
9	2000 Apr 4, 16:32	360	1188	N16, W60	...	...	N	55.8	0.321
10	2000 May 15, 16:26	>165	1212	S23, W68	...	...	N	1.86	...
11	2000 Jun 10, 17:08	360	1108	N22, W40	1.0	23.6	Y	46	6.25
12	2000 Jun 25, 7:54	165	1617	N10, W60	0.5	21.5	N	4.57	...
13	2000 Jun 28, 19:31	>134	1198	N24, W85	0.1	21.5	N	...	...
14	2000 Jul 14, 10:54	360	1674	N17, W2	...	...	N	24000	1670
15	2000 Sep 12, 11:54	360	1550	S14, W6	1.3	5.3	N	321	1.95
16	2000 Sep 16, 5:18	360	1215	N13, W6	0.2	16.2	Y	7.14	...
17	2000 Nov 8, 23:06	>170	1738	N14, W63	1.0	13.9	N	14800	1880
18	2000 Nov 24, 15:30	360	1245	N21, W12	...	...	N	94	4.98
19	2001 Feb 11, 1:31	360	1183	N21, W60	...	...	N	...	...
20	2001 Apr 2, 22:06	244	2505	N16, W65	...	...	N	1110	53.5
21	2001 Apr 9, 15:54	360	1192	S20, W4	0.3	29.0	Y	5.89	1.2
22	2001 Apr 10, 5:30	360	2411	S20, W10	0.3	29.0	Y	355	3.69
23	2001 Apr 12, 10:31	360	1184	S20, W43	0.3	29.0	Y	50.5	5.75
24	2001 Apr 15, 14:06	167	1199	S20, W85	0.3	29.0	Y	951	275
25	2001 Apr 26, 12:30	360	1006	N23, W2	0.9	15.5	Y	57.5	...
26	2001 Jul 19, 10:30	166	1668	S9, W61	0.4	23.3	Y	...	...
27	2001 Oct 1, 5:30	360	1405	S20, W89	1.6	11.5	N	2360	24.5
28	2001 Oct 22, 15:06	360	1336	S18, W20	0.6	30.5	Y	24.2	2.5
29	2001 Oct 25, 15:26	360	1092	S18, W20	0.5	30.5	Y	...	...
30	2001 Nov 4, 16:20	360	1274	N6, W18	...	...	N	31700	2120
31	2001 Nov 22, 23:30	360	1437	S17, W35	...	...	N	18900	162
32	2001 Dec 26, 5:30	>212	1446	N9, W61	0.7	12.6	Y	780	180
33	2002 Apr 17, 8:26	360	1218	N13, W12	0.8	12.0	Y	24.1	0.367
34	2002 Apr 21, 1:27	241	2409	S18, W79	...	...	N	2520	208
35	2002 May 22, 3:50	360	1494	S15, W70	0.9	17.6	N	820	1.15
36	2002 Jul 15, 20:30	360	1132	N20, W2	0.5	15.9	Y	234	0.92
37	2002 Jul 18, 8:06	360	1099	N20, W33	0.5	15.9	Y	14.2	0.635
38	2002 Aug 6, 18:25	134	1098	S38, W18	...	...	N	...	...
39	2002 Aug 14, 2:30	133	1309	N10, W60	0.6	10.1	N	26.4	...
40	2002 Aug 22, 2:06	360	1005	S14, W60	1.3	5.5	N	36.4	5.98
41	2002 Aug 24, 1:27	360	1878	S5, W89	1.2	5.5	N	317	76.2
42	2002 Nov 9, 13:31	360	1838	S9, W30	0.4	26.8	Y	404	1.46
43	2002 Dec 19, 22:06	360	1092	N16, W10	0.7	33.2	Y	4.22	...
44	2002 Dec 21, 2:30	225	1072	N30, W0	1.0	15.7	Y	...	...
45	2002 Dec 22, 3:30	272	1071	N24, W43	0.9	16.6	Y	...	...
46	2003 Mar 18, 12:30	209	1601	S13, W48	0.2	20.2	Y	0.84	...
47	2003 Mar 19, 2:30	360	1342	S13, W56	0.2	20.2	Y	...	...
48	2003 May 28, 00:50	360	1366	S5, W25	0.7	11.6	N	121	0.328
49	2003 May 31, 2:30	360	1835	S5, W65	0.7	11.2	N	27	2.33
50	2003 Oct 26, 17:54	>171	1537	N3, W43	0.4	42.0	Y	466	10.4
51	2003 Oct 27, 8:30	>215	1380	N3, W48	0.4	42.0	Y	52.0	9.59
52	2003 Oct 29, 20:54	360	2029	S16, W5	0.6	42.0	Y	2470	389
53	2003 Nov 2, 9:30	360	2036	S16, W51	0.7	34.0	Y	30.1	0.766
54	2003 Nov 2, 17:30	360	2598	S16, W56	0.7	34.0	Y	1570	155
55	2003 Nov 4, 19:54	360	2657	S16, W83	0.7	34.0	Y	353	15.3
56	2003 Nov 11, 13:54	360	1315	S3, W63	0.4	19.4	N	...	...

[a] Obtained from CME catalog (http://cdaw.gsfc.nasa.gov/CME_list).

[b] CME locations determined by the EIT movie.

[c] Shortest surface distance between a CME and a CH (from the CME site to the CH boundary) in units of $R_\odot$, called the CH proximity.

[d] Area of the closest CH in units of gr.

[e] Relative location of a CH to the corresponding CME. Y denotes a CH extending into the longitudes between the CME and the field lines connecting the Earth to the Sun at about W60°, and N denotes a CH outside the two longitudes.

[f] Peak fluxes of ≥10 MeV protons in units of pfu.

[g] Peak fluxes of ≥50 MeV protons in units of pfu.

& Jackson 1977; Fisher & Guhathakurta 1995; DeForest et al. 2001), and because the most efficient height of shock-accelerating SEPs is likely to be $\sim 3\ R_\odot$ (Cliver et al. 2004).

3. EIT 284 Å images of CHs are almost as informative as the soft X-ray emission (Moses et al. 1997; Chertok et al. 2002), which also has been widely used to study CHs.

The brightness of EUV emission recorded by EIT 284 Å contains the information of coronal density and temperature. The dark regions in EIT 284 Å images usually indicate CHs. Certainly, dimmings, which sometimes appear after CMEs (e.g., Zarro et al. 1999), and filaments may also be shown as dark regions. Thus, the EIT images taken before or long after CME onsets are used in order to avoid dimming regions, and Hα images are examined to distinguish filament-dark regions from CH-dark regions.

To determine the boundaries of dark regions, a method is developed by taking advantage of the brightness of the pixels in EIT 284 Å images. The following example from 2000 September 16 was used to describe the method (Fig. 1). Here, the CME occurred at 05:18 UT, so an EIT 284 Å image taken at 01:06 UT is chosen. In this image, each pixel has its own recorded brightness, b. For any given value of b, we can plot the contours and then calculate the area, A, enclosed by each contour. Many EIT 284 Å images show that brightness usually increases rapidly at CH boundaries in the direction from the center of the CH out. This is because magnetic fields are open in CHs and closed in the other regions. Such a difference should be evident in some physical parameters, including the detected brightness, much different between the inner and outer boundaries of CHs. Therefore, the derivation $f = \Delta b/\Delta A$ is used to determine the boundaries of dark regions. The potential CH boundaries are at the places where $f = f_{\max}$. By employing this brightness gradient method to this example, two large dark regions are outlined as indicated by the closed curves in Figure 1*a*. The areas of the two regions are $A = 16.2$ and 5.5 gr, with gr being the area of a $10^\circ \times 10^\circ$ grid as indicated by the mesh covering the solar surface in Figure 1*a*. Finally, filament-dark regions and small CHs ($A < 5$ gr) should be discarded. The two dark regions marked in this example are both large CHs.

As comparisons, Figures 1*b*–1*d* show the Kitt Peak CH map, the soft X-ray image from the *Yohkoh* SXT, and the magnetogram from the *SOHO* MDI. The Kitt Peak CHs were closer to the central meridian, as it was at 15:49 UT, 14 hours later than the EIT 284 Å image. Their shapes are similar to those of EIT 284 Å CHs except that the dark region near the north pole is not included. From the soft X-ray image, dark regions are very similar to the EIT 284 Å CHs, and the polar CH near the north pole is evident. The magnetogram from the *SOHO* MDI shows that the magnetic fields inside the two regions were all weak and monopolar, which are both the properties of a CH. This example suggests that the brightness gradient method can well determine CHs. The identified CHs are almost the same as those in soft X-ray images, but slightly different from the Kitt Peak CHs. Since CHs indeed look different at different spectra, we therefore call them EIT 284 Å CHs to distinguish our identified CHs from the others.

In this paper, all EIT 284 Å CHs are identified using the brightness gradient method. These CHs all look dark in EIT 284 Å images. In addition, two points should be noted. (1) This method reduces personal bias in the determination of CH boundaries. This is very important in a statistical study. (2) For some limb events, we use the EIT images in which CME locations were near the central meridian. Otherwise some CHs, which are very close to the CMEs but on the solar back-side at the time of CME onsets, cannot be identified.

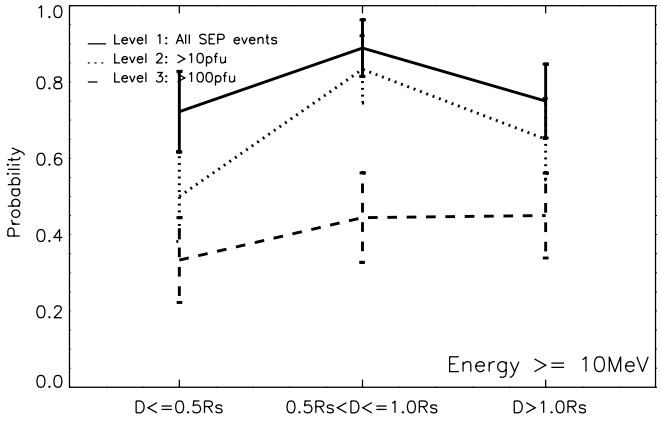

FIG. 2.—Occurrence probabilities, P, of SEP events vs. CH proximity, D, for proton energies $\geq$10 MeV. The probabilities at three flux levels (all SEP events, $\geq$10 and $\geq$100 pfu events, and 1 pfu = 1 particle cm^{-2} s^{-1} sr^{-1}) are indicated by solid, dotted, and dashed lines with error bars, respectively.

3. STATISTICAL RESULTS

SEP events can be affected by many factors. To examine whether there is any effect of CHs on SEP events, one should remove or reduce other impact factors as far as possible. A slow narrow CME cannot be considered a good producer of a SEP event and therefore cannot be used to study the CH effect. Moreover, SEP events evidently depend on CME longitude (Cane et al. 1988; Reames et al. 1996). A CME originating from the eastern hemisphere is less likely to create a SEP event near the Earth because of the magnetic connection between Sun and the Earth. Thus, we focus on the fast halo CMEs, which are also required to originate from the western hemisphere. The "fast" and "halo" mean that the CME projected speed measured in *SOHO* LASCO is larger than 1000 km s^{-1} and the span angle is larger than 130°.

On the basis of the CME catalog,[2] all the fast halo CMEs from 1997 to 2003 are investigated. A total of 97 fast halo CMEs are identified as definite *front-side* events, among which there were 62 western events. The SEP intensities are obtained from the profiles of 5 minute averaged proton integral fluxes by *Geostationary Operational Environmental Satellite* (*GOES*).[3] They are the peak fluxes during the increasing phase after CMEs' onset. Among the 62 western events, in six events the SEP intensities are difficult to be distinguished because their SEP fluxes were probably swamped by the more intense fluxes produced by earlier CMEs. Thus, the six events are excluded from our statistical study. The information for all the selected events is listed in Table 1. For the SEP column, the ellipses mean that there is no SEP event, for column A, no large ($\geq$5 gr) visible CH, and therefore for column D, no estimated CH proximity. It should be noted that "no visible CH" does not mean that no CH appeared on the Sun at that time. Perhaps there was a CH on the back-side, but we did not detect it. Thus, in our analysis, a large CH proximity of $D > 1.5\ R_\odot$ is given for the events without visible CHs. The locations listed in table are the CME initial/primary sites determined by examining EIT 195 Å movies (Wang et al. 2002). For example, the identified location of the CME on 2000 September 16 was about N13°, W6° (Fig. 1), and the nearest CH boundary lay at N24°, E2°, which was a distance of $\sim 0.2\ R_\odot$ away

[2] See http://cdaw.gsfc.nasa.gov/CME_list.
[3] See http://spidr.ngdc.noaa.gov.

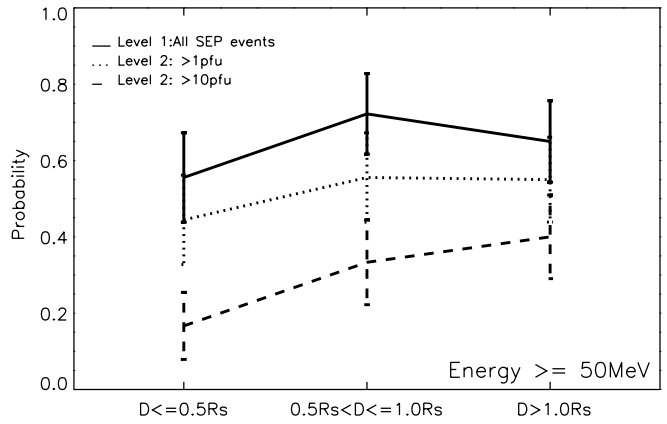

FIG. 3.—Occurrence probabilities of SEP events vs. CH proximity for proton energies ≥50 MeV.

from the CME location. One may notice that the measurement errors in the determination of CME locations cannot be avoided. However, it is easy to estimate that for a sample containing 54 events the standard error is about 0.02 $R_\odot$, which is much less than the precision of CH proximity applied in this paper. Thus, such measurement errors will not affect the statistical results significantly.

3.1. *Dependence on the CH Proximity*

First, we focus on the proton peak fluxes at energies ≥10 MeV, which are widely used to decide whether there is a (major) SEP event in space weather (e.g., by NOAA, Space Environment Center). Figure 2 shows the occurrence probabilities P of SEP events, i.e., the number ratios of SEP events to CMEs, versus CH proximity D. To get a reliable variation of SEP event probability with increasing CH proximity and avoid too large a standard deviation, we separate these events into three groups: small-proximity ($D \leq 0.5\ R_\odot$) events, moderate-proximity ($0.5\ R_\odot < D \leq 1.0\ R_\odot$) events, and large-proximity ($D > 1.0\ R_\odot$) events. Each group contains about 20 events according to Table 1. The probabilities at three flux levels (all SEP events, ≥10 and ≥100 pfu events, 1 pfu = 1 particle $cm^{-2}\ s^{-1}\ sr^{-1}$) are investigated as indicated by the different lines. The error bars approximately denote the one standard deviation (σ) level, which is calculated by $\sigma = [P(1-P)/N]^{1/2}$, where N is the number of CMEs.

Obviously, there is no clear dependence of SEP event probability on CH proximity. At each flux level, the probability is not monotonic as a function of D. It reaches the maximum at moderate proximity. Moreover, the error bars suggest that the variations of these probabilities are all significant at no more than 1 σ. Furthermore, there is no regularity in the probability variation as the flux level changes. Thus, the analysis of CH proximity on the sample suggests that CHs have no evident effect on CMEs in producing SEP events.

We further investigate the possibility that there is a CH effect on SEP events at higher energies, ≥50 MeV. The same analysis is performed. The results are shown in Figure 3. They are similar to Figure 2. There is still no evident CH effect found.

3.2. *Dependence on the CH Location*

Further, the possible impact of CH location relative to the corresponding CMEs is taken into account. Considering that magnetic field lines connecting Earth to the Sun are usually at about W60°, a CH extending into the longitudes between the Earth magnetic footpoint connection and the corresponding CME source region might cause the CME to have different behavior in producing SEP events. The shock produced by the CME as well as the possible accelerated SEPs must propagate through the intervening high-speed wind stream from the CH to the field lines connecting to the Earth. To investigate whether the relative location of CHs has influence on the production of SEPs, we divide these events into two groups as marked by "Y" and "N" in the third column of Table 1. The group marked by "Y" contains the events with CHs extending into the longitudes between the CME source and Earth magnetic connection on the Sun. Such CHs might separate CMEs from the magnetic field lines connecting to the Earth (hereafter called separating CHs). The group marked by "N" contains the events with CHs outside the two longitudes or without CHs (called outside-CH cases). It should be noted that for a polar CH, one cannot say whether it is outside the two longitudes or not. And from EIT images, it is also somewhat difficult to distinguish the longitude beyond the latitude of ±60° due to the project effect. Fortunately, in our sample, all the polar CHs extended to midlatitude. Thus, for a polar CH, we use the fraction of the CH within ±60° in latitude to determine its location relative to the corresponding CME.

The differences between these two CH groups in the formation of SEP events at various levels are exhibited in Figure 4. For all the events (Fig. 4*a*) and for distant CH events (Fig. 4*c*), the separating CH group (II) has a lower probability of producing SEP events than the outside CH group (I) at each SEP

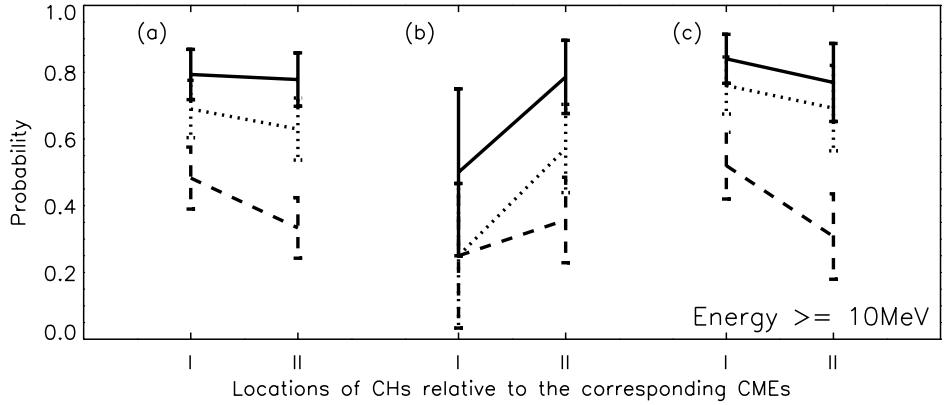

FIG. 4.—Comparison between the outside CH (I) and separating CH (II) cases in the occurrence probability of SEP events for proton energies ≥10 MeV. The different types of lines correspond to the three flux levels shown in Fig. 2. Parts (*a*), (*b*), and (*c*) represent all the events, the near CH ($D \leq 0.5\ R_\odot$) events, and the distant CH ($D > 0.5\ R_\odot$) events, respectively.

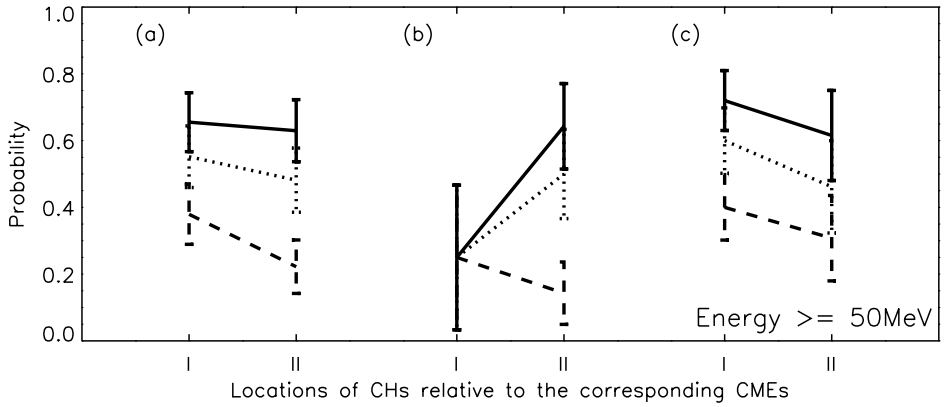

FIG. 5.—Comparison between the outside CH (I) and separating CH (II) cases in the occurrence probability of SEP events for proton energies $\geq$50 MeV. Parts (*a*), (*b*), and (*c*) and the line types are the same as those in Fig. 4.

flux level, but for the near-CH events (Fig. 4*b*), the separating CH group has slightly higher probability to produce SEP events. However, as noted in § 3.1, the uncertainties are too large for significance. None of the differences between the two groups exceeds 1 σ. This implies that the location of CHs relative to the corresponding CMEs has no evident effect on SEP events. Similarly, the analysis on the SEP events for proton energies $\geq$50 MeV is performed. Figure 5 shows the results, which also support the previous conclusion that no evident effect of CH location on SEP events exists.

4. SUMMARY AND CONCLUSIONS

In summary, a brightness gradient method is developed to identify CHs, in which personal bias is greatly reduced. By applying this method, the total of 56 front-side fast halo CMEs originating from the western hemisphere during 1997–2003 are investigated, as well as their associated CHs, and then the effect of CHs on CMEs in producing gradual SEP events is studied.

Our results show that neither CH proximity nor CH relative location exhibits any evident effect on the intensities of SEP events. Almost all of the statistical results do NOT have significance exceeding the 1 σ level. This is consistent with the previous conclusion suggested by Kahler (2004) that SEP events can be produced in fast solar wind regions and the associated CMEs are not required to be significantly faster than those in slow solar wind regions.

We acknowledge the use of the data from the *SOHO*, *Yohkoh*, and *GOES* spacecraft and the CH maps from the Kitt Peak Observatory. We express our heartfelt thanks to the anonymous referee for constructive suggestions and criticisms. *SOHO* is a project of international cooperation between ESA and NASA. This work is supported by the Chinese Academy of Sciences (KZCX3-SW-144 and startup fund), the National Natural Science Foundation of China (40525014, 40336052, 40574063, 40404014), and the Program for New Century Excellent Talents in University (NCET-04-0578).

REFERENCES

Bohlin, J. D. 1977, in Coronal Holes and High-Speed Wind Streams, ed. J. Zirker (Boulder: Colo. Univ. Press), 27
Cane, H. V. 1997, in Coronal Mass Ejections, ed. N. Crooker, J. A. Joselyn, & J. Feynman (Washington: AGU), 205
Cane, H. V., McGuire, R. E., & von Rosenvinge, T. T. 1986, ApJ, 301, 448
Cane, H. V., Reames, D. V., & von Rosenvinge, T. T. 1988, J. Geophys. Res., 93, 9555
Cane, H. V., von Rosenvinge, T. T., Cohen, C. M. S., & Mewaldt, R. A. 2003, Geophys. Res. Lett., 30, 5
Chertok, I. M., Obridko, E. I., Mogilevsky, V. N., Shilova, N. S., & Hudson, H. S. 2002, ApJ, 567, 1225
Cliver, E. W., Kahler, S. W., & Reames, D. V. 2004, ApJ, 605, 902
DeForest, C. E., Lamy, P. L., & Llebaria, A. 2001, ApJ, 560, 490
Delaboudiniere, J.-P., et al. 1995, Sol. Phys., 162, 291
Fainshtein, V. G. 2000, Adv. Space Res., 25, 1867
Fisher, R., & Guhathakurta, M. 1995, ApJ, 447, L139
Gopalswamy, N., Yashiro, S., Krucker, S., Stenborg, G., & Howard, R. A. 2004, J. Geophys. Res., 109, 12105
Gopalswamy, N., Yashiro, S., Michalek, G., Xie, H., Lepping, R. P., & Howard, R. A. 2005, Geophys. Res. Lett., 32, 12
Harvey, K. L., & Recely, F. 2002, Sol. Phys., 211, 31
Kahler, S. W. 2001, J. Geophys. Res., 106, 20947
———. 2004, ApJ, 603, 330
Kahler, S. W., & Hundhausen, A. J. 1992, J. Geophys. Res., 97, 1619
Kahler, S. W., & Reames, D. V. 2003, ApJ, 584, 1063
Kallenrode, M.-B. 2003, J. Phys. G, 29, 965
Moses, D., et al. 1997, Sol. Phys., 175, 571
Munro, R. H., & Jackson, B. V. 1977, ApJ, 213, 874
Reames, D. V. 1997, in Coronal Mass Ejections, ed. N. Crooker, J. A. Joselyn, & J. Feynman (Washington: AGU), 217
———. 1999, Space Sci. Rev., 90, 413
———. 2000, in AIP Conf. Proc. 516, 26th International Cosmic Ray Conference, ed. B. L. Dingus, D. B. Kieda, & M. H. Salamon (Melville: AIP), 289
Reames, D. V., Barbier, L. M., & von Rosenvinge, T. T. 1996, ApJ, 466, 473
Wang, Y., Shen, C., Wang, S., & Ye, P. 2004, Sol. Phys., 222, 329
Wang, Y. M., Ye, P. Z., Wang, S., Zhou, G. P., & Wang, J. X. 2002, J. Geophys. Res. 107, 2
Zarro, D. M., Sterling, A. C., Thompson, B. J., Hudson, H. S., & Nitta, N. 1999, ApJ, 520, L139
Zhao, X. P., Hoeksema, J. T., & Scherrer, P. H. 1999, J. Geophys. Res., 104, 9735